Impact of VR Educational Games on Users: A Classification Algorithm Based on EEG Signal Feature Extraction

Ying Zhao [1]*, Guocheng Wei [2]

[1]School of Humanities, Laboratory of Humanities, Wenzhou University, Wenzhou Zhejiang, 325000, China
[2]Maoteng Mao Teng E-commerce Company, Wenzhou Zhejiang, 325000, China

*Corresponding author e-mail: 00101085@wzu.edu.cn

Abstract. Attention has a significant impact on cognitive abilities including learning and deciding. Under the fast growth of internet technology, virtual reality has also greatly progressed. Exploring the impact of virtual reality games on attention is of great importance, but quantitative analysis on the influence of virtual games on attention is inadequate. To address this issue, a method based on support vector machines is invented to judge and classify electroencephalography signals. Firstly, a method based on wavelet thresholding and ensemble empirical mode decomposition is proposed to address the problem of difficult extraction and processing of electroencephalography signals. This method can preprocess the real-time electroencephalography signals collected from users in different attention states, and then classify the signals using an improved support vector machines. Experiment outcomes told that when the training set size is 500, the root mean square error values of the wavelet thresholding method, ensemble empirical mode decomposition, and hybrid algorithm are 0.25, 0.19, and 0.16. The values of the hybrid algorithm for the alpha, beta, theta, and delta frequency bands are 0.09, 0.15, 0.19, and 0.11, respectively. When the dataset size is 800, the root mean square error values of the convolutional neural network model, support vector machines model, and improved support vector machines model are 0.19, 0.16, and 0.13, respectively. The research results indicate that the proposed hybrid denoising algorithm and improved support vector machines model have good model performance, providing theoretical support for attention training and testing in fields such as psychology and education.

Keywords: Virtual reality games, Attention, Ensemble empirical mode decomposition, Support vector machines

1 Introduction

Under the fast growth of internet, virtual reality (VR) has made significant progress, allowing VR games to create more realistic scenarios [1]. Currently, the diagnosis of brain waves generally involves the use of scales combined with electroencephalogram

K. Chulsoo et al. (eds.), *Proceedings of the 2025 4th International Conference on Art Design and Digital Technology (ADDT 2025)*, Advances in Computer Science Research 123,
https://doi.org/10.2991/978-94-6463-815-8_70

(EEG) graphs. Biomedical research has shown that the fluctuations in EEG signals can reflect the brain's activity state [2]. When the trend of power spectral density decreases, it indicates that certain brain functions are insufficiently awakened, resulting in power not being the main component of electrical activity. The external manifestation is the difficulty in completing the process of attention. Currently, the judgment of attention status mainly relies on doctors' interpretation of EEG graphs. For this study, a Long Short Term Memory (LSTM) based solution is proposed to judge and classify EEG signals. Firstly, to address the problem of difficult extraction and processing of EEG signals, a wavelet thresholding based solution with Ensemble Empirical Mode Decomposition (EEMD) is given. This method can preprocess the real-time EEG signals collected from users in different attention states, and then classify the signals using an improved LSTM. The content in the study is categorized as four main parts. The first provides an overview of other scholars' research on signal feature extraction. The second part presents a review of the methods used in this study. The third part presents the results obtained from applying the methods and analyzes the results. The fourth part summarizes all the research and provides prospects for future studies.

2 Related Works

Attention refers to the direction and concentration of mental activity or consciousness towards a specific object. It can be understood as the ability to focus consciousness, indicating the degree of attention. Z. Yu et al. found that the connectivity between multiple brain regions in mental fatigue has not been thoroughly studied, and the commonly used methods based on EEG wave connectivity analysis are unable to overcome strong noise interference. Therefore, the research team proposed an adaptive feature extraction model based on stacked denoising autoencoders. This method can extract features with a high signal-to-noise ratio (SNR) and suppress noise interference. Experimental results show that compared to principal component analysis, the proposed method significantly improves the SNR and suppresses noise interference [3].J. G. Wang et al. found that under brain-computer interfaces and electrode technology growth, there have been many studies on emotion recognition based on EEG graphs. The research team proposed a new emotion recognition model based on EEG waves, which uses a convolutional neural network to classify three emotions: positive, neutral, and negative. This method constructs the model by directly inputting EEG wave data, ensuring the integrity of information utilization. The experiment outcomes told that the method recognize emotions [4].

In summary, many scholars have conducted research on EEG signal recognition and have achieved certain results. However, no scholar has introduced virtual games in the study of EEG waves. For this study, a Support Vector Machines (SVM) based method is proposed to judge and classify EEG signals. Firstly, to address the problem of difficult extraction and processing of EEG signals, a method based on wavelet thresholding and ensemble empirical mode decomposition is proposed. This method can preprocess the real-time EEG signals collected from users in different attention states, and then classify the signals using an improved support vector machine.

3 Research on EEG Signal Feature Extraction and Classification Algorithms

In the first section of this chapter, a method based on wavelet thresholding and ensemble empirical mode decomposition is proposed, which can preprocess real-time EEG signals collected from users in different attention states. In the second section, SVM is proposed and improved for signal classification.

3.1 Research on EEG Signal Analysis Methods

EEG waves refer to the fluctuating signals generated by the electrical activity in the human brain, which can be recorded and analyzed through EEG graphs. Brain-computer interaction allows people to interact directly with brain activity, enabling communication and control with external devices without the need for traditional physical movements [5]. Brain-computer interaction technology is based on the acquisition and analysis of EEG physiological signals such as EEG waves, brain magnetic waves, or brain oxygenation. By using these signals, it is possible to recognize and interpret brain activities such as intentions, thoughts, and emotions, and convert them into control commands, enabling interaction with computers, robots, prosthetics, wheelchairs, and other devices. In this study, a non-invasive interface was used to acquire EEG signals through a brain-computer interface. This method is convenient, risk-free, and does not cause neural damage to the subjects. However, due to the interference of the scalp and other tissues, the signal noise is high, and the spatial and temporal resolution of the signals is relatively low, which may eventually let decreased signal accuracy and precision appear. The EEG signal states obtained through non-invasive brain-computer interfaces can objectively reflect the level of attention of individuals. The EEG feature rhythms corresponding to different brain activity states are given in Table 1.

Table 1. Characteristics of Four Rhythms

EEG wave	Corresponding state
α (8-13Hz)	Appears when awake, relaxed, quiet, and with eyes closed
β (13-32Hz)	When quiet and closed, it only appears in the frontal lobe area, and when opening, thinking, or receiving other stimuli, it also appears in other cortical areas.
θ (4-8Hz)	Appears when fatigue or central nervous system is in a suppressed state.
δ (1-4Hz)	It may appear during sleep, but not during wakefulness. In addition, it is also more common in the EEG waveform of some patients with brain diseases.

From Table 1, it can be seen that α EEG waves appear when the brain is relatively inactive, such as during wakefulness, relaxation, and quietness. β EEG waves appear in the frontal lobe area when in a quiet or closed-eye state, and may also appear in other cortical areas when thinking or stimulated. θ EEG waves appear during fatigue or when the central nervous system is inhibited [6]. δ EEG waves only appear during sleep. The acquired EEG signals through non-invasive brain-computer interfaces need to be processed by amplifiers and converted into digital information. The EEG signal analysis process is shown in Figure 1.

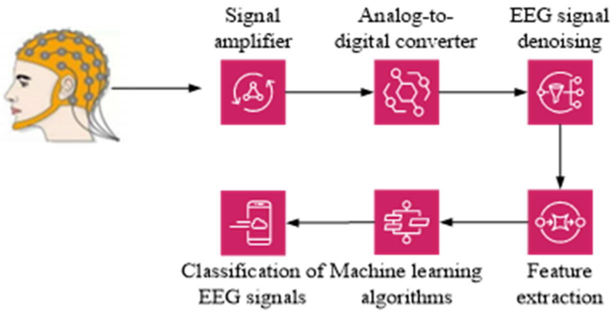

Fig. 1. EEG signal analysis process.

From Figure 1, it can be seen that EEG wave signals are collected through a non-invasive brain-computer interface. Due to the transmission of these signals through the scalp and other tissues, and the interference from various sources of noise, the collected data needs to be processed by a signal amplifier and then converted into digital signals through an analog-to-digital converter. During the process of collecting EEG wave signals, denoising is required to obtain clean EEG signals. Attention-related EEG features are then extracted, followed by classification using traditional machine learning solutions. Due to the extremely weak nature of EEG signals acquired through non-invasive brain-computer interfaces and the complexity of neuronal activity during brain-computer interaction, various interferences are often encountered during the EEG signal acquisition process. These interferences can significantly affect the acquired EEG signals. Therefore, a method combining ensemble empirical mode decomposition and wavelet thresholding is used for denoising EEG signals. Wavelet thresholding is a commonly used signal processing method that can be applied in the preprocessing of non-invasive interface signals such as EEG graphs [7]. This solution is supported by wavelet transform, which decomposes the signal into different frequency subbands and removes noise by setting a threshold. The expression is shown in Equation (1).

$$W_f(a,\tau) = \left\langle f, \psi_{a,b} \right\rangle = \frac{1}{\sqrt{a}} \int_{-\infty}^{+\infty} f(t) * \varphi(\frac{t-\tau}{a}) dt \tag{1}$$

In Equation (1), a represents frequency, τ represents time, $\psi_{a,b}$ represents the wavelet basis function, and $\varphi(t)$ represents the phase function. By controlling a and τ, the scaling and translation of the wavelet function can be controlled. Attention-related EEG signals are generally low-frequency signals or in specific frequency bands, while noise in the original signal is in high-frequency bands. Based on this characteristic, combined with the differences in time and frequency of different frequency bands in wavelet transform, the EEG signals are processed.

Additionally, wavelet transform can discover the sparsity and decorrelation of signals to ensure the effectiveness of the processed EEG signals. The process of wavelet thresholding denoising consists of three steps: first, the noisy signal is decomposed using wavelet transform; then, the wavelet coefficients are thresholded; finally, the wavelet coefficients of each layer are reconstructed. The key point of wavelet thresholding denoising is the selection of the threshold function. Traditional thresholds are generally categorized as hard and soft thresholding methods. The wavelet hard thresholding denoising method is shown in Equation (2).

$$\widetilde{W_{j,k}} = \begin{cases} 0 & ,\left|W_{j,k}\right| \le \lambda \\ W_{j,k}, & \left|W_{j,k}\right| > \lambda \end{cases} \tag{2}$$

In Equation (2), $W_{j,k}$ represents the denoised data, and λ represents the denoising threshold. The wavelet soft thresholding denoising method is shown in Equation (3).

$$\widetilde{W_{j,k}} = \begin{cases} 0 & ,\left|W_{j,k}\right| \le \lambda \\ \operatorname{sgn}(W_{j,k})(\left|W_{j,k}\right| - \lambda), & \left|W_{j,k}\right| > \lambda \end{cases} \tag{3}$$

However, both of the above methods have different degrees of problems. The hard thresholding method has signal oscillation issues, while the soft thresholding method has constant error. To address this problem, the empirical mode decomposition (EMD) method is introduced to improve the model. The EMD basic idea is decomposing the signal into a set of local oscillatory modes, each mode having different frequencies and amplitudes. These modes are called intrinsic mode functions (IMF). The decomposition of the original signal requires the following conditions: first, the oscillation frequencies of the IMFs are locally equal in the entire signal, meaning that the IMFs are locally frequency-adjusted, and the average values at any moment are zero. The decomposition formula that satisfies these conditions is shown in Equation (4).

$$x(t) = \sum_{i=1}^{n} imf_i(t) + r_n \tag{4}$$

In Equation (4), $x(t)$ represents the original signal, $imf_i(t)$ represents the IMF, and r_n represents the residue. First, the local max and minima original signal are confirmed, and the upper and lower envelopes are plotted. The new sequence is acquired via subtracting the mean of the upper and lower envelopes from the original signal, and this process is repeated until no further decomposition is possible [8]. When the occurrence of extreme points in the EEG signal is relatively random, the IMF components will have approximate scale component signal distributions in different IMFs, resulting in mode mixing.

Therefore, the EEMD algorithm is used, and its process is shown in Figure 2.

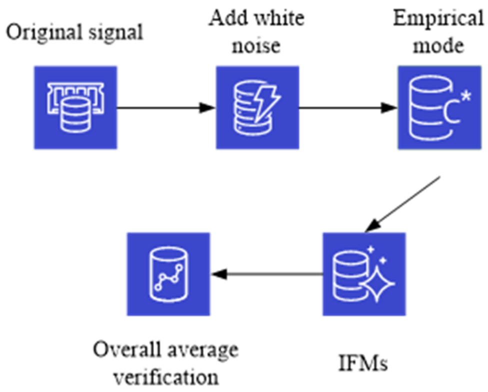

Fig. 2. EEMD Algorithm Flowchart.

From Figure 2, it can be seen that white noise sequences are added to the original signal, and different items are added each time. After obtaining a set of IMF, the results are averaged. The noise data will cancel each other out after multiple averaging calculations, and the final output is the denoised result. The combined denoising process of the two methods is shown in Figure 3.

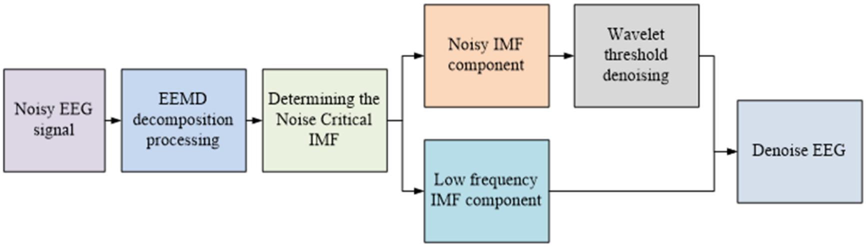

Fig. 3. Flow chart of EEMD and improved wavelet threshold denoising.

From Figure 3, it can be seen that the first step is to determine the critical IMF components containing noise. The energy density of the IMF after EEMD decomposition of the initial signal is constant when multiplied by the average period. The calculation method for energy density of the original signal is shown in Equation (5).

$$EN_i = \frac{1}{n}\sum_{j=1}^{n} imf_{i,j}^2 \tag{5}$$

In Equation (5), EN_i represents the energy density of the i -th IMF component, imf represents the intrinsic mode function, and n represents the length of each

IMF component. The calculation method for the average period is shown in Equation (6).

$$\overline{T} = \frac{2n}{D_i} \tag{6}$$

In Equation (6), D_i represents the number of extreme points in the i-th IMF component. If the mean of the IMF satisfies the condition of being an integer multiple of a certain size, the first k IMF components are the main noisy modes. Then, the improved wavelet thresholding is applied to denoise the first k IMF components [9]. To address the drawbacks of soft and hard thresholding, targeted improvements are made, and the improved algorithm is shown in Equation (7).

$$\widetilde{W_{j,k}} = \begin{cases} 0 & ,\left|W_{j,k}\right| \le \lambda \\ \operatorname{sgn}(W_{j,k})(\left|W_{j,k}\right| - \frac{\lambda}{e^{W_{j,k}^2-\lambda^2}}), & \left|W_{j,k}\right| > \lambda \end{cases} \tag{7}$$

In Equation (7), $W_{j,k}$ represents the denoised data, and λ represents the denoising threshold. The reconstructed signal is shown in Equation (8).

$$\begin{cases} \lim\limits_{W_{j,k} \to +\infty} \frac{\widetilde{W_{j,k}}}{W_{j,k}} = 1 - \frac{\lambda W_{j,k}}{e^{W_{j,k}^2-\lambda^2}} = 1, W_{j,k} > 0 \\ \lim\limits_{W_{j,k} \to +\infty} \frac{\widetilde{W_{j,k}}}{W_{j,k}} = 1 + \frac{\lambda W_{j,k}}{e^{W_{j,k}^2-\lambda^2}} = 1, W_{j,k} < 0 \\ \lambda = \sigma\sqrt{2\ln N} \end{cases} \tag{8}$$

In Equation (8), N represents the length of the sequence, and σ represents the standard deviation of the noisy signal. For the improved threshold function, as $W_{j,k}$ increases, the value of $\frac{\lambda}{e^{W_{j,k}^2-\lambda^2}}$ gradually decreases.

3.2 Research on EEG Classification Algorithm Based on Attention Features

Power spectrum estimation is a solution used for analyzing the spectral characteristics of a signal, typically used to determine the frequency distribution and energy distribution of a signal. This method can help understand the frequency components, frequency characteristics, and energy distribution of a signal. In this study, the smoothed averaged periodogram method is used to analyze EEG signals under different attention states [10].

The smoothed averaged periodogram method is a power spectrum estimation that performs Fourier transform and averaging on multiple segments of a signal. Compared to other solutions, the smoothed averaged periodogram method has three advantages, as shown in Figure 4.

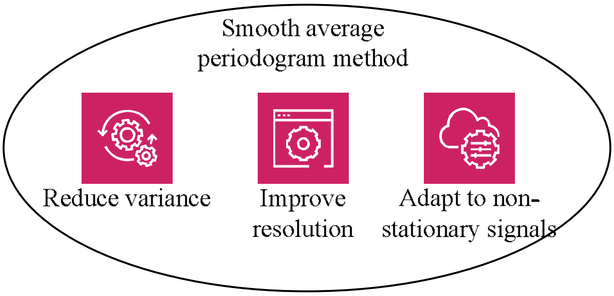

Fig. 4. Advantages of the smoothed averaged periodogram method.

The first advantage is variance reduction. By averaging multiple segments of a signal, the smoothed averaged periodogram method can effectively reduce the variance of the estimated power spectrum. Since signals are often affected by noise, the power spectrum estimation obtained from a single Fourier transform may have significant fluctuations. By averaging multiple segments of the signal, the fluctuations can be reduced, resulting in more stable and reliable power spectrum estimation results [11]. The second advantage is improved resolution. The smoothed averaged periodogram method performs Fourier transform on multiple segments of the signal and averages the obtained spectra. This improves the resolution of the power spectrum estimation, making the frequency components more clear and distinguishable. Compared to power spectrum estimation obtained from a single Fourier transform, the smoothed averaged periodogram method can better reveal the frequency characteristics of the signal[12]. The third advantage is adaptability to non-stationary signals. The smoothed averaged periodogram method is suitable for power spectrum estimation of non-stationary signals. For non-stationary signals, their frequency characteristics may change over time. By segmenting the signal, performing Fourier transform, and averaging, the smoothed averaged periodogram method can better capture the frequency distribution of the signal in different time periods, meeting the analysis needs of non-stationary signals. The mathematical formula for this method is shown in Equation (9).

$$S(w)=\frac{1}{k}\sum_{i=1}^{k}\frac{\left|\sum_{N=0}^{M-1}X^{i}(n)w(n)e^{-j\frac{2\pi}{N}kn}\right|}{\sum_{N=0}^{M-1}w^{2}(n)} \tag{9}$$

In Equation (9), N represents the number of data points, K represents the number of segments, $X(n)$ represents the segmented data, and $w(n)$ represents the window function. Although this method can intuitively reflect the power distribution of the four rhythms, it still has certain limitations. This method can only analyze the energy characteristic changes involving the four frequency bands in the EEG signal. Therefore, further quantification of each rhythm is needed. Autoregressive modeling is introduced for quantification. Autoregressive modeling is a statistical model commonly used for time series modeling. This model assumes a correlation between the current value of the sequence and past values, using past observations to predict future observations [13]. In the autoregressive model, the current observation is considered as a linear combination of past observations, where the coefficients at each time point represent the influence of past observations on the current observation. The expression is shown in Equation (10).

$$x(n) = -\sum_{i=1}^{p} a_p(i)x(n-i) + \varepsilon(n) \tag{10}$$

In Equation (10), $x(n)$ represents the EEG sequence, $\varepsilon(n)$ represents white noise. The calculation formula for estimating the autoregressive model parameters using the Burg method is shown in Equation (11).

$$\begin{cases} P = \frac{1}{2}(P_f + P_b) \\ P_f = \frac{1}{M-k}\sum_{n=k}^{M-1}\left|e_k^f(n)\right|^2 \\ P_b = \frac{1}{M-k}\sum_{n=k}^{M-1}\left|e_p^b(n)\right|^2 \end{cases} \tag{11}$$

In Equation (11), P_f represents the forward error power, P_b represents the backward error power, and P represents the sum of error powers. After applying this equation to estimate the auto-regressive power spectrum of the EEG signal, the mean of the obtained power spectrum data is used as a feature point [14]. The data features are further analyzed using the sample entropy algorithm, which is defined in Equation (12).

$$SampEn = -\ln\left[A^k(r) / B^k(r)\right] \tag{12}$$

In Equation (12), r represents the estimated similarity, which is a real number. $A^k(r)$ and $B^k(r)$ represent the similarity probabilities between two vectors. After performing EEMD decomposition on the signal, the obtained components are then subjected to Hilbert transform, which is defined in Equation (13).

$$\begin{cases} H[x(t)] = h(t) * x(t) = \int_{-\infty}^{+\infty} x(\tau)h(t-\tau)d\tau = \dfrac{1}{\pi}\int_{-\infty}^{+\infty} \dfrac{x(\tau)}{t-\tau}d\tau \\ h(t) = \dfrac{1}{\pi t} \\ x(t) = A(t)e^{j\varphi(t)} \end{cases} \tag{13}$$

In Equation (13), $H[x(t)]$ represents the Hilbert transform, $x(t)$ represents the original signal, A represents the amplitude, e represents the phase, $h(t)$ represents the impulse response function, and $A(t)$ represents the amplitude function. After data processing, classification is required. In this study, SVM is used for EEG signal classification, with the radial basis function as the kernel function, as shown in Equation (14).

$$k(x,x_i) = \exp - \left|x - x_i\right|^2 / \sigma^2 \tag{14}$$

In Equation (14), x_i represents the center point, x represents the input variable, and $\left|x - x_i\right|^2$ represents the squared Euclidean distance between each input value in the function and the center point x_i. However, in the case of a large dataset, the training speed of this method is slightly slow. Therefore, the LSTM network is introduced to improve the SVM feature classification algorithm. LSTM is a type of Recurrent Neural Network (RNN) architecture used for processing sequential data. Compared to traditional RNNs, LSTM introduces gate mechanisms that can better capture long-term dependencies [15]. In traditional RNNs, information is passed through consecutive time steps, but as the number of time steps increases, the information may gradually vanish or be overwritten, which is known as the vanishing gradient and exploding gradient problems. LSTM solves this problem by using gate units to effectively retain and propagate important information, with the core being the internal memory of the cell. The cell state can be passed along the time steps and selectively updated or ignored. The structure of an LSTM neuron is shown in Figure 5.

From Figure 5, it can be seen that the LSTM neuron structure adds gate structures to the RNN, including the input gate, forget gate, and output gate. Compared to RNN, LSTM has an additional state called the cell state, which consists of a long-term state and a short-term state [16]. Taking the unit at time t as the object, the calculation formulas for each layer in the LSTM network are shown in Equation (15).

$$\begin{cases} g_i = \tanh(W_{xg}^T \cdot x_t + W_{hg}^T \cdot h_{t-1} + b_g) \\ i_i = \sigma(W_{xi}^T \cdot x_t + W_{hi}^T \cdot h_{t-1} + b_i) \\ f_i = \sigma(W_{xf}^T \cdot x_t + W_{hf}^T \cdot h_{t-1} + b_f) \\ i_i = \sigma(W_{xo}^T \cdot x_t + W_{ho}^T \cdot h_{t-1} + b_o) \end{cases} \tag{15}$$

In Equation (15), W represents the weight matrix between layers, represents the hyperbolic tangent function, b represents the bias term, σ represents the sigmoid function, g_t represents the main layer in the LSTM network, i_t represents the forget gate control, f_t represents the input gate control, and o_t represents the output gate control [17]. The flowchart of the attention-based EEG signal classification algorithm based on LSTM-SVM is shown in Figure 6.

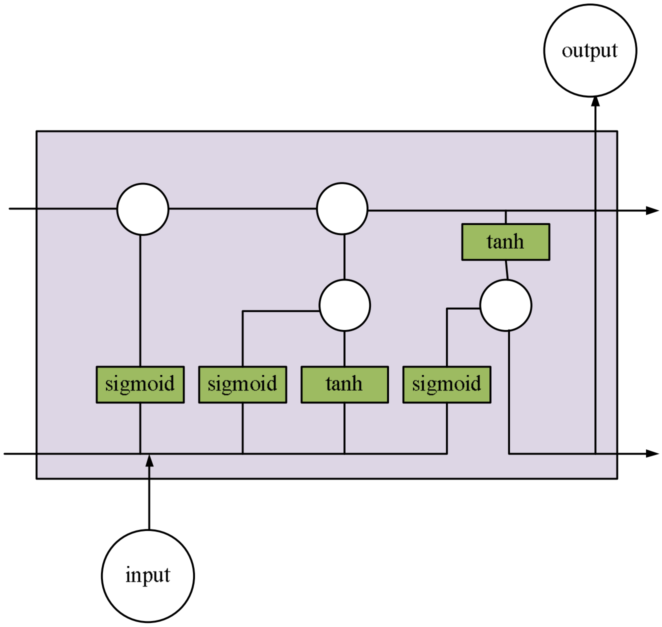

Fig. 5. Details of LSTM neuron structure.

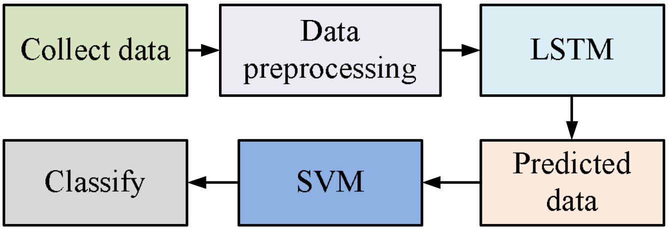

Fig. 6. Flowchart of the attention-based EEG signal classification algorithm based on LSTM-SVM.

From Figure 6, it can be seen that the first step is to collect EEG signals, preprocess the collected signals, then input the data into the LSTM model to obtain the predicted data, and finally input it into the SVM model to obtain the output result.

4 Performance Analysis of EEG Signal Feature Extraction and Classfication Algorithms

In the first section of this chapter, the wavelet thresholding method and EEMD were introduced. The proposed hybrid algorithm was compared based on SNR, root mean square error (RMSE), denoising ability in different EEG frequency bands, and model processing time. In the second section of this chapter, RNN and SVM algorithms were introduced, and the models were compared based on accuracy and RMSE.

4.1 Performance Analysis of EEG Signal Denoising Models

This study was trailed on a system with an Intel(R) Core(TM) i5-10210U CPU, 20GB RAM, Windows 10 operating system, and 8GB memory. The wavelet thresholding method, EEMD, and the hybrid denoising method proposed in this study were compared. The SNR and RMSE of the three methods were shown in Figure 7.

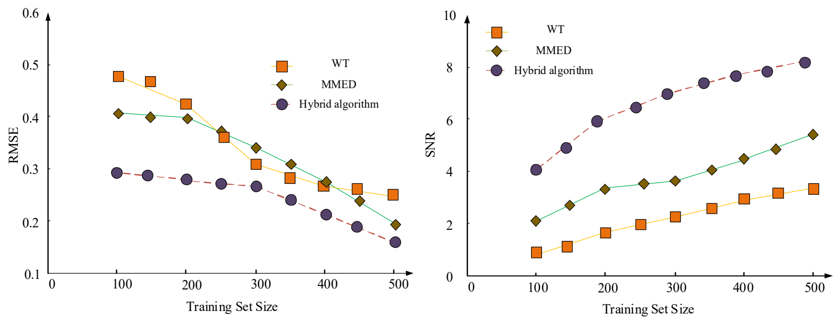

(a)Changes in RMSE of different algorithm models in training sets

(b)Changes in SNR of different algorithm models in the training set

Fig. 7. Comparison of RMSE and SNR for different algorithms.

Figure 7(a) showed the variation of RMSE for different algorithm models in the training set, and Figure 7(b) showed the variation of training SNR. From Figure 7(a), it could be observed that as the training set size increased, the RMSE values of the three algorithm models decreased, and the hybrid model proposed in this study had the lowest RMSE value among the three models. When the training set size was 500, the RMSE values for the wavelet thresholding method, EEMD, and the hybrid algorithm were 0.25, 0.19, and 0.16, respectively. From Figure 7(b), it could be observed that as the size of the training set increased, the SNR of each model increased. When the training set size was 500, the SNR values for the wavelet thresholding method, EEMD, and the hybrid algorithm were 3.7, 5.4, and 8.2, respectively. Among the three algorithms, the hybrid algorithm had a significantly higher SNR. The experimental results indicated that as the size of the training set increased, the RMSE values of the wavelet thresholding method, EEMD, and the hybrid algorithm decreased, and the SNR values increased. Among the three algorithms, the proposed hybrid algorithm performed significantly better in terms of denoising ability. The denoising abilities of the three algorithms in different frequency bands of EEG waves generated by users during VR educational games were compared, and the outcomes were given in Figure 8.

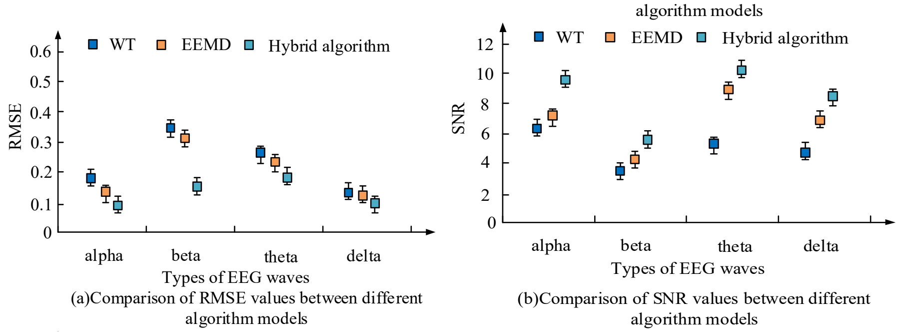

Fig. 8. Comparison of denoising information for different EEG frequency bands generated during VR educational games using three algorithms.

Figure 8(a) showed the comparison of RMSE values for different EEG frequency bands using the three algorithms, and Figure 8(b) showed the comparison of SNR values for different EEG frequency bands using the three algorithms. From Figure 8(a), it could be observed that among the four frequency bands, the three methods had higher RMSE values for the beta band, which was due to the complexity of the EEG waves in the beta band. The hybrid algorithm had RMSE values of 0.09, 0.15, 0.19, and 0.11 for the alpha, beta, theta, and delta bands, respectively. From Figure 8(b), among the four frequency bands, the three methods had lower SNR values for the beta band. The proposed hybrid algorithm had SNR values of 9.7, 5.8, 10.3, and 8.7 for the alpha, beta, theta, and delta bands, respectively. The experimental results indicated that the wavelet thresholding method and ensemble empirical mode decomposition method had poor denoising ability for beta waves, but performed well in other EEG bands. The proposed hybrid denoising model exhibited good denoising ability in all types of EEG waves. The denoising time of the three models for different frequency bands of EEG waves generated during VR educational games was compared, and the results were shown in Figure 9.

From Figure 9, it could be observed that in the alpha band, the denoising time for the WT denoising algorithm model, EEMD denoising algorithm model, and hybrid algorithm model were 3.6s, 2.3s, and 3.1s, respectively. In the beta band, the denoising time for the three algorithm models were 4.2s, 2.9s, and 3.2s, respectively. In the theta band, the denoising time for the three algorithm models were 3.8s, 2.6s, and 2.9s, respectively. In the delta band, the denoising time for the three algorithm models were 3.8s, 2.6s, and 2.9s, respectively. The experimental results indicated that among the four EEG frequency bands, the beta band took longer time for denoising due to its complexity, while the other bands were relatively simpler and required less time for denoising compared to the beta band. Among the three models, the proposed hybrid algorithm model had shorter denoising time, indicating good performance of the proposed one. Fifty professionals were randomly selected and divided into five groups to rate the denoising methods proposed in this study. The outcomes were shown in Table 2.

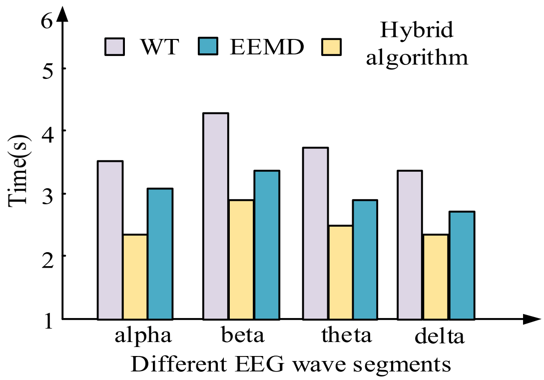

Fig. 9. Denoising time for different algorithms and EEG frequency bands.

Table 2. Performance evaluation of denoising models

Model type	Group 1	Group 2	Group 3	Group 4	Group 5
Hybrid algorithm	87.2	92.8	95.6	84.5	91.6
EEMD	85.1	85.9	91.6	78.4	86.5
WT	79.8	80.7	87.5	74.1	78.6

From Table 2, it could be observed that the evaluation scores for the hybrid model by the five groups were 87.2, 92.8, 95.6, 84.5, and 91.6. The evaluation scores for the ensemble empirical mode decomposition method by the five groups were 85.1, 85.9, 91.6, 78.4, and 86.5. The evaluation scores for the wavelet thresholding method by the five groups were 79.8, 80.7, 87.5, 74.1, and 78.6. The experiment outcomes told that the evaluation scores for the hybrid algorithm model by the five groups were relatively high, suggesting that the proposed algorithm model had good performance.

4.2 Performance Analysis of EEG Classification Algorithms Based on Attention Features

After determining the hybrid algorithm as the denoising model, the performance of the classification model needed to be compared. In this study, the SVM and RNN were introduced and compared with the proposed LSTM-SVM algorithm model. The outcomes were shown in Figure 10.

Figure 10(a) showed the RMSE values of the three algorithms for different dataset sizes, and Figure 10(b) showed the accuracy of the three algorithms for different datasets. From Figure 10(a), as the dataset size increased, the RMSE values of the three models decreased. When the dataset size was 800, the RMSE values for the RNN model, SVM model, and LSTM-SVM model were 0.19, 0.16, and 0.13, respectively. From Figure 10(b), as the dataset size increased, the accuracy of the three models improved, with the LSTM-SVM algorithm model achieving higher accuracy. The experimental results indicated that the proposed LSTM-SVM algorithm had good model accuracy. Fifty users were randomly selected, and the performance of the three algorithm models under different user states during VR gameplay was compared. The results were shown in Figure 11.

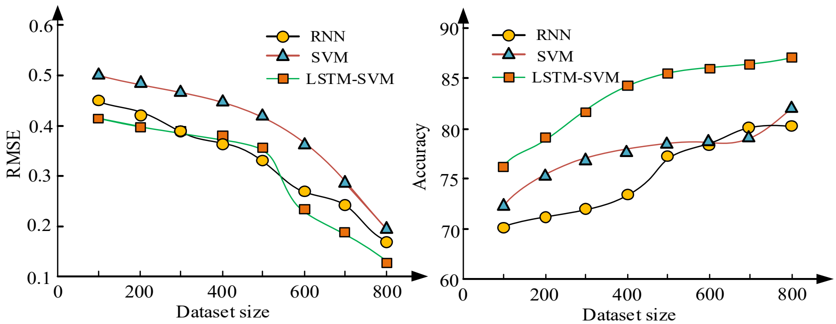

(a)Comparison of RMSE values between different models

(b)Comparison of accuracy between different models

Fig. 10. Performance comparison of different algorithms.

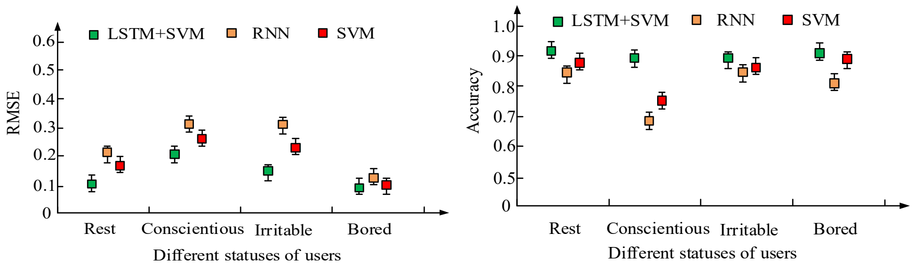

(a)Comparison of RMSE values between different algorithm models

(b)Comparison of Accuracy between different algorithm models

Fig. 11. Performance of different models under different user states.

Figure 11(a) showed the comparison of RMSE values for different user states during gameplay. Figure 11(b) showed the comparison of accuracy for different user states during gameplay. From Figure 11, it could be observed that the RNN model and SVM model had lower RMSE and accuracy under the focused and agitated states, which was due to the complexity of the EEG waves in these states. The LSTM-SVM model achieved higher accuracy under different user states. The experiment outcomes told that the proposed LSTM-SVM model could handle various complex EEG wave conditions. The processing time of the three algorithms for EEG waves generated by users during VR educational games was compared, and the results were shown in Figure 12.

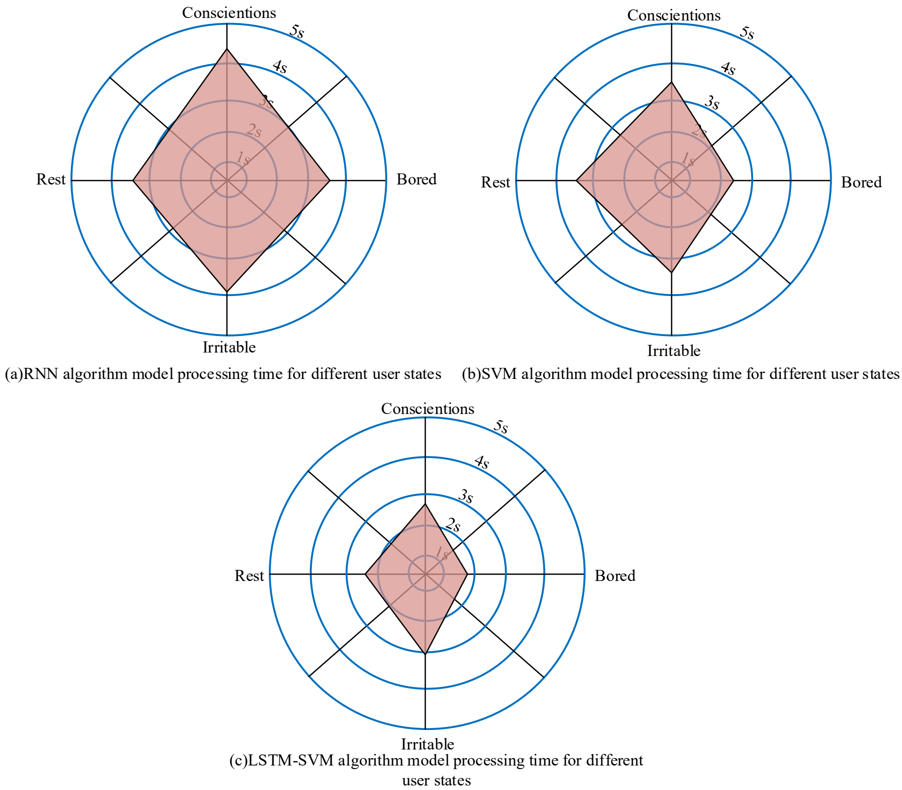

Fig. 12. Model processing time under different user states.

Figure 12(a), Figure 12(b), and Figure 12(c) represented the processing time of the RNN, SVM, and LSTM-SVM algorithms under different user states, respectively. From the figures, it could be observed that the RNN algorithm model had processing times of 3.5s, 4.3s, 3.9s, and 3.4s for users in the resting, focused, anxious, and bored states, respectively. The SVM algorithm model had processing times of 3.4s, 3.5s, 3.4s, and 2.5s for users in the resting, focused, anxious, and bored states, respectively. The LSTM-SVM algorithm model had processing times of 2.4s, 2.7s, 3.1s, and 1.7s for users in the resting, focused, anxious, and bored states, respectively. The experiment outcomes told that the proposed one had good recognition and classification efficiency for users in different states. Fifty users were randomly selected and divided into five groups, and their EEG waves during gameplay were classified, and the matching degree with their own states was evaluated. The oucomes were shown in Table 3.

Table 3. User evaluation table

Model type	Group 2	Group 3	Group 4	Group 5
LSTM-SVM	87.8	92.6	94.5	82.6
SVM	85.9	84.4	87.4	81.5
RNN	76.7	81.2	74.1	72.5

From Table 3, it could be observed that the evaluation scores for the LSTM-SVM algorithm model by the five groups were 95.2, 87.8, 92.6, 94.5, and 82.6. The evaluation scores for the SVM algorithm model were 87.1, 85.9, 84.4, 87.4, and 81.5. The evaluation scores for the RNN algorithm model were 82.8, 76.7, 81.2, 74.1, and 72.5. The experimental results indicated that the proposed algorithm model had good user evaluation.

5 Conclusion

The core of the study on the impact of VR games on attention is to determine the method for evaluating attention. A SVM-based solution is proposed to judge and classify EEG signals. Firstly, to address the difficulty in extracting and processing EEG signals, a wavelet thresholding based solution with EEMD is invented. Then, SVM is improved for signal classification. The experimental results show that when the training set size is 500, the SNRs of the wavelet thresholding method, EEMD method, and hybrid algorithm model are 3.7, 5.4, and 8.2, respectively. Among the three algorithms, the hybrid algorithm has a much higher SNR than the other two. In the alpha band, the denoising time of the WT denoising algorithm model, EEMD denoising algorithm model, and hybrid algorithm model are 3.6s, 2.3s, and 3.1s, respectively. In the beta band, the denoising time of the models are 4.2s, 2.9s, and 3.2s, respectively. In the theta band, the denoising time of the models are 3.8s, 2.6s, and 2.9s, respectively. In the delta band, the denoising time of the models are 3.8s, 2.6s, and 2.9s, respectively. When the dataset size is 800, the RMSE values of the RNN model, SVM model, and LSTM-SVM model are 0.19, 0.16, and 0.13, respectively. The NN model and SVM model have lower RMSE and accuracy under the focused and agitated states, while the LSTM-SVM model achieves higher accuracy under different states. Fifty users were randomly selected and divided into five groups, and the evaluation scores for the LSTM-SVM algorithm model by the five groups are 95.2, 87.8, 92.6, 94.5, and 82.6. The evaluation scores for the SVM algorithm model are 87.1, 85.9, 84.4, 87.4, and 81.5. The evaluation scores for the RNN algorithm model are 82.8, 76.7, 81.2, 74.1, and 72.5. The research results indicate that the proposed model has good ability in attention classification. The research results also show that the proposed algorithm model has good performance and can provide theoretical support for attention training and testing in fields such as medicine and education. However, there are still limitations in the study. Due to the low sampling frequency of EEG acquisition devices, the attention states cannot be divided into more categories based on the existing collection methods. In the future, improvements in the collection methods can be considered to allow for more classifications.

Acknowledgment

The research is supported by: National First-class Undergraduate Courses in Virtual Simulation Experiment (No. 2020120160); Province Zhejiang Virtual Simulation Experiment Teaching Project (No. 2019276).

References

1. E. Fernandez-Blanco, D. Rivero, and A. Pazos, "EEG signal processing with separable convolutional neural network for automatic scoring of sleeping stage," *Neurocomputing*, vol. 410, no. 10, pp. 220-228, Oct. 2020. DOI:10.1016/j.neucom.2020.05.085.
2. Y. Wang, R. Behroozmand, L. P. Johnson, L. Boniha, and J. Fridriksson, "Topological signal processing and inference of event-related potential response," *J. Neurosci. Methods*, vol. 363, no. 10, pp. 109-124, Nov. 2021. DOI:10.1016/j.jneumeth.2021.109324.
3. Z. Yu, L. Li, W. Zhang, H. Lv, Y. Lin, and U. Khalique, "An adaptive EEG feature extraction method based on stacked denoising autoencoder for mental fatigue connectivity," *Neural. Plast.*, vol. 5, no. 7, pp. 1-12, Jan. 2021. DOI:10.1155/2021/3965385.
4. J. G. Wang, H. M. Shao, Y. Yao, J. L. Liu, H. P. Sun, and S. W. Ma, "Electroencephalograph-based emotion recognition using convolutional neural network without manual feature extraction," *Appl. Soft. Comput.*, vol. 128, no. 4, pp. 153-163, Oct. 2022. DOI:10.1016/j.asoc.2022.109534
5. M. Saini, U. Satija, and M. D. Upadhyay, "Wavelet based waveform distortion measures for assessment of denoised EEG quality with reference to noise-free EEG signal," *IEEE Signal Process. Lett.*, vol. 99, no. 4, pp. 9-12, Jul. 2020. DOI:10.1109/LSP.2020.3006417.
6. S. Bhalerao, I. A. Ansari, and A. Kumar, "Protection of BCI system via reversible watermarking of EEG signal," *Electron. Lett.*, vol. 56, no. 25, pp. 1389-1392, Dec. 2020. DOI:10.1049/el.2020.2532.
7. C. Chaiyanan, K. Iramina, and B. Kaewkamnerdpong, "Investigation on identifying implicit learning event from EEG signal using multiscale entropy and artificial bee colony," *Entropy*, vol. 23, no. 5, pp. 617-621, May 2021. DOI:10.3390/e23050617.
8. A. Olamat, P. Ozel, and S. Atasever, "Deep learning methods for multi-channel EEG-based emotion recognition," *Int. J. Neural Syst.*, vol. 32, no. 5, pp. 225-232, May 2022. DOI:10.1142/S0129065722500216.
9. C. C. Liu, S. G. Hajra, S. D. Fickling, G. Pawlowski, X. Song, and R. C. N. D'Arcy, "Novel signal processing technique for capture and isolation of blink-related oscillations using a low-density electrode array for bedside evaluation of consciousness," *IEEE Trans. Biomed. Eng.*, vol. 67, no. 2, pp. 453-453, Feb. 2020. DOI:10.1109/tbme.2019.2915185.
10. S. Phadikar, N. Sinha, and R. Ghosh, "Automatic eyeblink artefact identification and removal from EEG using independent component analysis in combination with support vector machines and denoising autoencoder," *IET Signal Proc.*, vol. 14, no. 6, pp. 396-405, Aug. 2020. DOI:10.1049/iet-spr.2020.0025.
11. H. Qin and P. Sampsa, "An extended application 'Brain Q' processing EEG and MEG data of finger stimulation extended from 'Zeffiro' based on machine learning and signal processing," *Cognit. Syst. Res.*, vol. 65, no. 21, pp. 50-66, Oct. 2021. DOI:10.1016/j.cogsys.2020.08.006.

12. Q. Lin, S. Song, I. D. Castro, H. Jiang, M. Konijnenburg, and R. Wegberg, "Wearable multiple modality bio-signal recording and processing on chip: a review," *IEEE Sens. J.*, vol. 21, no. 2, pp. 1108-1123, Jan. 2020. DOI:10.1109/JSEN.2020.3016115.
13. T. Xu, Y. Zhou, Z. Hou, and W. Zhang, "Decode brain system: a dynamic adaptive convolutional quorum voting approach for variable-length EEG data," *Complexity*, vol. 2020, no. 20, pp. 118-123, Mar. 2020. DOI:org/10.1155/2020/6929546.
14. H. Wang, H. Guo, K. Zhang, L. Gao, and J. Zhang, "Automatic sleep staging method of EEG signal based on transfer learning and fusion network," *Neurocomputing*, vol. 488, no. 7, pp. 183-193, Jun. 2022. DOI:10.1016/j.neucom.2022.02.049.
15. Y. Xu, C. Hu, Q. Wu, S. Jian, and Z. Li, "Research on particle swarm optimization in LSTM neural networks for rainfall-runoff simulation," *J. Hydrol.*, vol. 608, no. 14, pp. 171-183, May 2022. DOI:10.1016/j.jhydrol.2022.127553.
16. L. Che, Y. Zuo, and L. Zhang, "Application of three-layer stacked LSTM model assisted by educational robots in children's learning," *Int. J. Humanoid Rob.*, vol. 19, no. 3, pp. 89-107, Jun. 2022. DOI:10.1142/S0219843622400114.
17. F. Masood, J. Masood, H. Zahir, K. Driss, N. Mehmood, and H. Farooq, "Novel approach to evaluate classification algorithms and feature selection filter algorithms using medical data," J. Comput. Cogn. Eng., vol. 2, no. 1, pp. 57-67, Nov. 2023. DOI:10.47852/bonviewJCCE2202238.